Human Rad51 filaments on double- and single-stranded DNA: correlating regular and irregular forms with recombination function

Dejan Ristic[1], Mauro Modesti[1], Thijn van der Heijden[2], John van Noort[2], Cees Dekker[2], Roland Kanaar[1,3] and Claire Wyman[1,3,*]

[1]Department of Cell Biology and Genetics, Erasmus Medical Center, PO Box 1738, 3000 DR Rotterdam, The Netherlands, [2]Kavli Institute of Nanoscience, Delft University of Technology, Lorentzweg 1, 2628 CJ Delft, The Netherlands and [3]Department of Radiation Oncology, Erasmus Medical Center-Daniel, Rotterdam, The Netherlands

ABSTRACT

Recombinase proteins assembled into helical filaments on DNA are believed to be the catalytic core of homologous recombination. The assembly, disassembly and dynamic rearrangements of this structure must drive the DNA strand exchange reactions of homologous recombination. The sensitivity of eukaryotic recombinase activity to reaction conditions *in vitro* suggests that the status of bound nucleotide cofactors is important for function and possibly for filament structure. We analyzed nucleoprotein filaments formed by the human recombinase Rad51 in a variety of conditions on double-stranded and single-stranded DNA by scanning force microscopy. Regular filaments with extended double-stranded DNA correlated with active *in vitro* recombination, possibly due to stabilizing the DNA products of these assays. Though filaments formed readily on single-stranded DNA, they were very rarely regular structures. The irregular structure of filaments on single-stranded DNA suggests that Rad51 monomers are dynamic in filaments and that regular filaments are transient. Indeed, single molecule force spectroscopy of Rad51 filament assembly and disassembly in magnetic tweezers revealed protein association and disassociation from many points along the DNA, with kinetics different from those of RecA. The dynamic rearrangements of proteins and DNA within Rad51 nucleoprotein filaments could be key events driving strand exchange in homologous recombination.

INTRODUCTION

Homologous recombination, the exchange of strands between homologous DNA molecules, is a universal aspect of genome metabolism needed to repair DNA double-strand breaks, to ensure proper replication and chromosome segregation and to create genetic diversity. The defining mechanistic steps of homologous recombination are DNA strand invasion and joint molecule formation. These reactions are catalyzed by a class of proteins called recombinases, typified by bacterial RecA, and including the RadA homologs in archaea and the Rad51 homologs in eukaryotes. The recombinase proteins all assemble into helical nucleoprotein filaments on DNA. The nucleoprotein filaments formed by bacterial RecA were first observed more than two decades ago (1–3). Since then, this filament structure has proven to be highly conserved. Recombinases from all three kingdoms of life assemble on both single-stranded and double-stranded DNA into very similar filaments despite the limited conservation among their amino acid sequences [structures reviewed in (4)]. Current models of homologous recombination involve strand exchange occurring within the recombinase nucleoprotein filament. The mechanistic details of homology search and the exchange of DNA strands are currently obscure, but must require dynamic rearrangements of the nucleoprotein filament involving both DNA and the recombinase proteins.

The *in vitro* activity of the eukaryotic recombinases is sensitive to a number of reaction conditions suggested to affect protein or filament conformation related to ATP binding (5–8). The status of bound nucleotide cofactors influences DNA binding for both RecA and Rad51, though in subtly different ways for the recombinases from different organisms (9–14). The formation of a recombination-competent nucleoprotein filament in all cases requires a bound nucleotide cofactor.

Conversely, ATP hydrolysis by the recombinases is dependent on their interaction with DNA, with single-stranded DNA stimulating the activity more strongly than double-stranded DNA (15,16). However, the mechanistic role of ATP hydrolysis in recombination remains enigmatic. ATP hydrolysis is dispensable for RecA and Rad51 catalyzed *in vitro* recombination reactions, which assess the pre-synaptic and synaptic stages of recombination, including homology search, strand invasion and joint molecule formation (7,17,18). However, based on the phenotypes of ATPase defective recombinases, *in vivo* recombination does require ATP hydrolysis (19–21).

Here, we described the effect of reaction conditions that influence *in vitro* recombination on the structure of human Rad51 nucleoprotein filaments. The filaments were observed directly in the absence of fixatives and characterized with scanning force microscopy (SFM). In conditions that enhance *in vitro* recombination activity, we observed regular and stable filaments with elongated double-stranded DNA. Filaments formed on single-stranded DNA were almost all irregular in all conditions unless they were fixed with glutaraldehyde. In contrast, Rad51 filaments on double-stranded DNA were irregular and apparently unstable in conditions where *in vitro* recombination activity is low. Disassembly of filaments was followed over time revealing that protein disassociation occurs from many places along the filament. Single molecule force spectroscopy studies of Rad51 filament assembly and disassembly also showed that stable filaments form in conditions that favor *in vitro* strand exchange reactions. Furthermore, the kinetics of filament disassembly followed in solution in real-time indicated dissociation of Rad51 subunits from many points at once.

MATERIALS AND METHODS

DNA substrates

The double-stranded DNA used in the SFM experiments was made by linearization of pDERI1 (22). Digestion of this plasmid with ScaI produced 1821 bp blunt-ended linear double-stranded DNA. The resulting linear DNA was purified by phenol:chloroform:iso-amyl alcohol (25:24:1) extraction and checked for purity by gel electrophoresis.

A sample of 810 nt single-stranded DNA was made as follows: first a double-stranded 810 bp fragment was produced by PCR, using the URA3 gene from *Saccharomyces cerevisiae* as template DNA and primers U3, which was 5′-phosphorylated (5′-GAAGGAAGAACGAAGGAAGGAGC), and Bio 5, which was 5′ biotinylated (5′-TTTCCCGGGGGG-CCCGGGTTCTATACTGTTGACCC). The PCR product was purified by phenol:chloroform:iso-amyl alcohol (25:24:1) extraction, followed by ethanol precipitation. The DNA strand with the terminal 5′-phosphate was digested by lambda exonuclease (5 U/µg DNA). The reaction was carried out at 37°C for 1 h and stopped by the addition of a 0.1 vol of STOP solution containing 5% (w/v) SDS, 50 mM EDTA, 30 mg/ml Proteinase K and further incubation at 65°C for 30 min. The resulting single-stranded DNA was resolved on a 1.5% agarose gel and purified from the gel using a GFX™ column (Amersham).

For the magnetic tweezers experiments, freely rotatable 8 kb DNA was made as described previously (23).

Rad51 purification

The human Rad51 protein was over-expressed in *Escherichia coli*. Cells were lysed in high salt. The clarified lysate was treated with polyethylenimine. After a second clarification, Rad51 was recovered by $(NH_4)_2SO_4$ salting-out and the resuspended pellet was purified by heparin-sepharose chromatography followed by MonoQ chromatography. The protein was dialyzed against 300 mM KCl, 20 HEPES–NaOH (pH 7.8), 1 mM EDTA, 2 mM DTT and 10% glycerol, and stored at $-80°C$.

Filament formation reactions

Nucleoprotein filaments were formed in 10 µl reactions containing 7.5 µM DNA (concentration in nucleotides), 2.5 µM human Rad51, 25 mM HEPES–KOH (pH 7.5), 5 mM $MgCl_2$ or $CaCl_2$, 2 mM nucleotide cofactor (ATP, ADP, ATPγS or AMP-PNP) and 30 mM KCl. Reactions were carried out at 37°C for 1 h and then placed on ice. When indicated, 200 mM $(NH_4)_2SO_4$ was added after 1 h of incubation at 37°C which was continued for an additional 10 min prior to placing the reactions on ice.

D-loop assays

Oligonucleotide SK3 (24) was radiolabeled at the 5′ end and incubated at 3.6 µM (nucleotide) with 1.6 µM Rad51 in 50 mM Tris–HCl (pH 7.5), 1 mM DTT, 0.1 mg/ml acetylated BSA, 60 mM KCl, 5 mM $MgCl_2$ (or $CaCl_2$) and 2 mM ATP (or AMP-PNP or ATPγS). After 5 min incubation at 37°C, 10 µl of supercoiled pUC19 plasmid DNA at 1.14 mM nucleotide (prepared by detergent lysis and twice purified by CsCl gradient equilibrium sedimentation) was added. At the desired time point, 10 µl aliquots were withdrawn from the reaction, mixed with 5 µl of STOP solution (0.5% SDS, 50 mM EDTA and 30% glycerol) and deproteinized by incubation for 5 min at 37°C with 1 µg/µl final of Proteinase K. Reaction products were fractionated by 0.8% agarose gel electrophoresis in Tris–borate buffer. Gels were dried on DEAE paper and analyzed by Phosphorimaging.

Scanning force microscopy

For imaging, reactions were diluted 15-fold in deposition buffer [10 mM HEPES–KOH (pH 7.5) and 10 mM $MgCl_2$] and deposited on freshly cleaved mica. After ~30 s, the mica was washed with water (glass distilled; SIGMA) and exposed to a stream of filtered air.

For the study of human Rad51 disassembly on mica, nucleoprotein filaments were formed as described above including treatment with $(NH_4)_2SO_4$. Reactions were deposited on mica and the excess buffer was removed, but the samples were not dried. The sample on mica was then covered with buffer containing 25 mM HEPES–KOH (pH 7.5), 5 mM $MgCl_2$, 2 mM ATP and 30 mM KCl, or 200 mM $(NH_4)_2SO_4$. The nucleoprotein filaments were incubated at 19°C for 1, 5 or 30 min and then washed and dried as described above.

Images were obtained on a NanoScope IIIa or a NanoScope IV (Digital Instruments; Santa Barbara, CA) operating in tapping mode in air with a type E scanner. Silicon Nanotips were purchased from Digital Instruments (Nanoprobes). The length of nucleoprotein filaments was measured from NanoScope images imported into IMAGE SXM 1.62 (National Institutes

of Health IMAGE version modified by Steve Barrett, Surface Science Research Centre, University of Liverpool, Liverpool, UK). The filaments' contours were traced manually. For the irregular filaments, the contours were traced as a path through the highest points along the nucleoprotein filaments.

Magnetic tweezers

The magnetic tweezers setup used has been described in (25). The force applied to the bead was calculated by quantifying thermal motion of the DNA-tethered bead and substituting it into equipartition theorem. Using image processing, a position accuracy of 5 nm in three dimensions was obtained. To exclude thermal drift, all positions were measured relative to a polystyrene bead fixed to the bottom of the flow cell. Length changes of a magnitude up to 10 nm or with a frequency <30 Hz could be determined reliably within the spatial and temporal noise for Z detection at the force used.

Polystyrene beads, as well as DNA constructs carrying a magnetic bead at one end, were anchored to the bottom of a flow cell as described (25). Force-extension curves were used to identify attachment of single DNA molecules. After conformation of the correct contour and persistence lengths, experiments were started by addition of human Rad51. All measurements were carried out at 25°C.

Flow cell reactions

The reaction buffer used in the flow cell was 25 mM HEPES–KOH (pH 7.5), 5 mM $MgCl_2$ and 25 mM KCl. For the start of a measurement, the flow cell content was replaced by buffer including human Rad51 and 2 mM ATP while maintaining the DNA tether at a constant magnetic force. Note however that due to the flow (first 60–75 s), an additional drag force pulls on the bead. As a result, the bead is moved sideways and downwards, increasing the tether length, but decreasing the bead height. Human Rad51 (dis)assembly was monitored through measurement of the height of the magnetic bead.

RESULTS

The structure of nucleoprotein filaments formed by the human recombinase Rad51 was analyzed by SFM imaging. In this way, we not only assessed if the protein binds to DNA under the conditions tested, but also directly observed the architecture of the resulting protein–DNA complexes. Significantly, sample preparation does not require fixative agents thereby allowing the observation of possibly dynamic structures. This approach also resulted in capturing for observation the variety of structures present in a reaction mixture at the time of deposition. Comparing unfixed and fixed filaments indicated that chemical fixation forced the accumulation of regular structures.

Human Rad51 formed regular and irregular filaments on double-stranded DNA depending on reaction conditions

Nucleoprotein filaments formed in the presence of ATP and Mg^{2+} on 1.8 kb double-stranded DNA were irregular and varied in length (Figure 1A). To assess DNA extension in the filaments, their contour length was measured by tracing

a path through the highest points along the protein–DNA complex. This was compared to the contour length of DNA molecules in the absence of protein measured in the same way. All length measurements are displayed as distributions in histograms (Figure 2). The length of the filaments formed in the presence of ATP and Mg^{2+} indicated that many of the DNA molecules were not significantly extended in these complexes (Figure 2A and B). The filaments with lengths significantly shorter than the 1.8 kb DNA (average measured length 0.53 μm) were due to contaminating short DNA fragments that were eliminated in subsequent experiments. Filaments formed in the presence of ATPγS, a nucleotide cofactor analog usually described as poorly hydrolyzable, were similar to those formed with ATP, irregular (Figure 1B) and without DNA extension.

Dramatically different filaments formed in the presence of the non-hydrolyzable ATP analog AMP-PNP (Figure 1D). Here, there were very few filaments with intermediate lengths between that of the bare 1.8 kb fragment (0.53 μm) and the fully extended length (0.8 μm), expected if the DNA is completely incorporated into a filament making it 1.5 times longer (Figure 2D). These filaments were regular and, apart from the filaments formed on the small contaminating DNA, had a uniform length indicating extension of the DNA to ~1.5 times that of a B-form.

In addition to varying the nucleotide cofactor, we also formed Rad51 filaments in buffer conditions known to influence the *in vitro* strand exchange reactions. Rad51-catalyzed strand exchange is stimulated by the addition of ammonium sulfate to a reaction including ATP and Mg^{2+} (8) and the (partial) substitution of Ca^{2+} for Mg^{2+} in an ATP-containing reaction (7). Filaments were formed as described above by addition of protein and nucleotide cofactor to DNA, where ammonium sulfate was added subsequently. These conditions, both addition of ammonium sulfate (Figure 1C) and substitution of Ca^{2+} for Mg^{2+} (Figure 1E), resulted in filaments with a regular appearance, similar to those formed in the presence of AMP-PNP. Addition of ammonium sulfate resulted in elongated filaments, though with a distribution centered at shorter than fully extended length (Figure 2C). Careful inspection of images of these filaments suggests their less than complete extension may be due to less than complete coverage of DNA by Rad51, but where DNA is covered the structures are regular (see apparent gaps in filaments shown in Figure 1C). Substitution of Ca^{2+} for Mg^{2+} resulted in filaments with a length distribution centered near the fully extended form (Figure 2E).

Human Rad51 rarely formed regular filaments on single-stranded DNA

We also analyzed the structure of Rad51 filaments formed on single-stranded DNA, the complex that initiates joint molecule formation and is presumably active in identifying regions of sequence homology. Rad51 was incubated with single-stranded DNA, a natural plasmid sequence ~800 nt long, in the same set of conditions and the same protein to DNA ratio (equivalent here to one Rad51 monomer per 3 nt of DNA) as was done for double-stranded DNA. In the absence of protein cross-linking agents, regular filaments were only rarely observed. Filaments were classified as regular or irregular
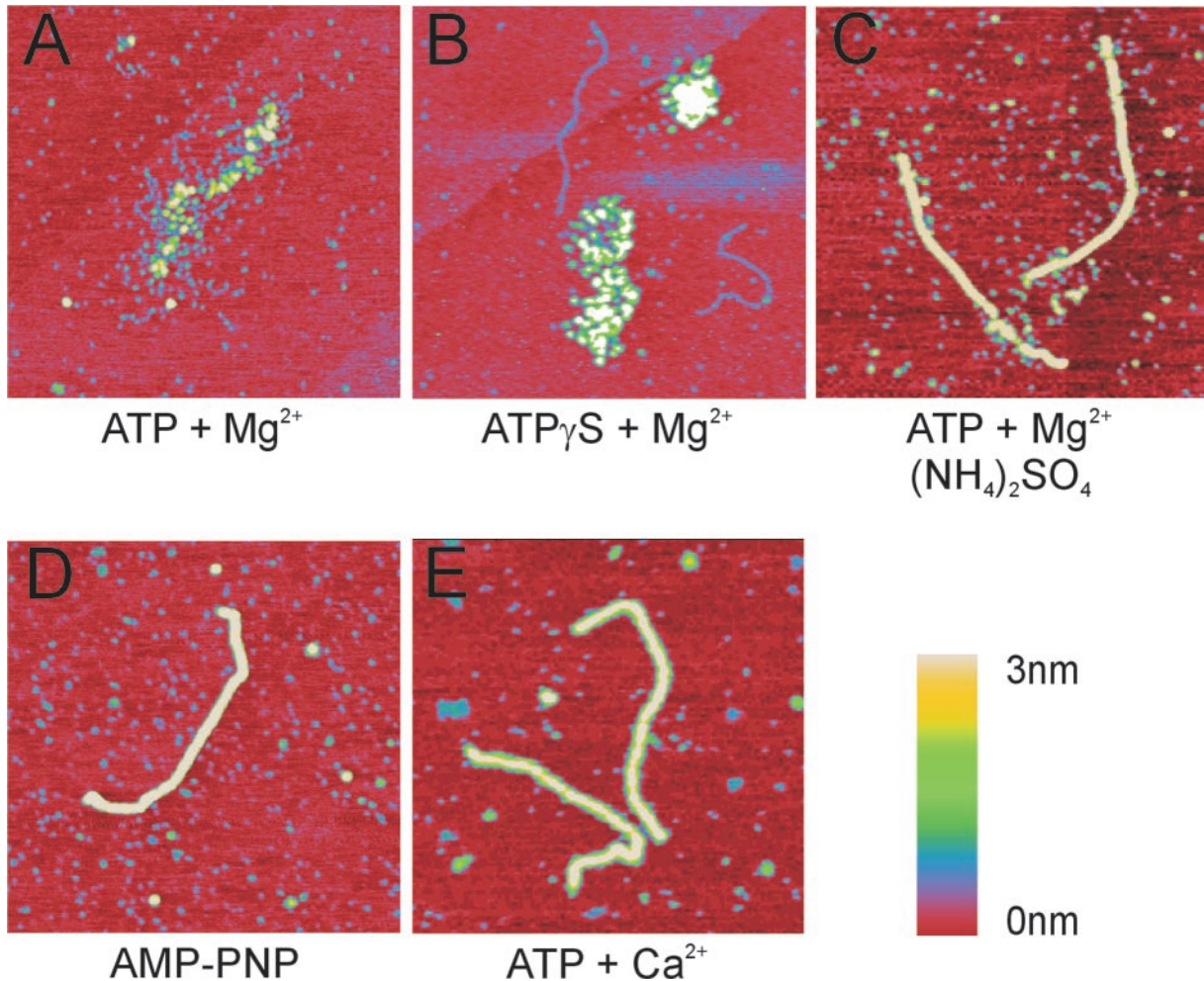
Figure 1. SFM images of filaments formed by human Rad51 on double-stranded DNA in the presence of various nucleotide cofactors. (**A** and **B**) Examples of protein–DNA complexes described as irregular filaments formed on double-stranded DNA in the presence of ATP and $MgCl_2$ (A) and ATPγS (B). (**C**–**E**) Examples of regular filaments formed on double-stranded DNA in conditions including ATP and $MgCl_2$ treated with $(NH_4)_2SO_4$ (C), AMP-PNP (D) and ATP and $CaCl_2$ (E). All images are 1×1 μm and height is represented by color in the range of 0–3 nm, red to yellow as shown in the scale bar.

based on their appearance and the percentage of regular and irregular filaments in the various conditions was tabulated (Figure 3). Regular or partially regular filaments were observed when ATP in the presence of Ca^{2+} or AMP-PNP was used as a nucleotide cofactor. For AMP-PNP, only a small fraction of the filaments were regular (85%, $n = 60$, of the filaments were irregular, see example in Figure 3D). Filaments formed in the presence of ATP and Ca^{2+} were occasionally like those formed on double-stranded DNA and classified as regular (Figure 3E). However, most of them had an intermediate appearance, not completely regular but not as irregular as filaments formed, for instance, with ATP and Mg^{2+} (compare Figure 3A and C with Figure 3E). All other conditions resulted in irregular filaments. Notably, the addition of ammonium sulfate to filaments formed with ATP and Mg^{2+} caused apparent disassociation of protein from DNA in the irregular filaments present before addition of ammonium sulfate. However, treatment of the reactions producing irregular filaments with glutaraldehyde resulted in all of the filaments becoming regular (compare Figure 3A and B). This suggests that the irregular structures observed on mica were a sampling

of dynamic filaments in solution with subunits rearranging or associating and disassociating. Fixation by glutaraldehyde may have trapped a structure that was only transiently present or that was the sum of dynamic interactions that occur in the time the cross-linking agent was present.

Human Rad51 recombination activity varied with reaction conditions

The structure of Rad51 filaments varied based on the DNA substrate and the reaction conditions. The conditions used were previously described to effect *in vitro* recombination activity, but have not all been directly compared in the same assay. In order to correlate filament structure with activity directly, we tested all of these conditions with our Rad51 protein in a D-loop assay (Figure 4). As judged by D-loop product accumulation, Rad51 is most active in the presence of AMP-PNP or ATP and Ca^{2+}. Indeed, in these conditions product signal at the time labeled 0 (Figure 4) indicated that product was formed in even the very short time it took to remove an aliquot after mixing all components. Only weak
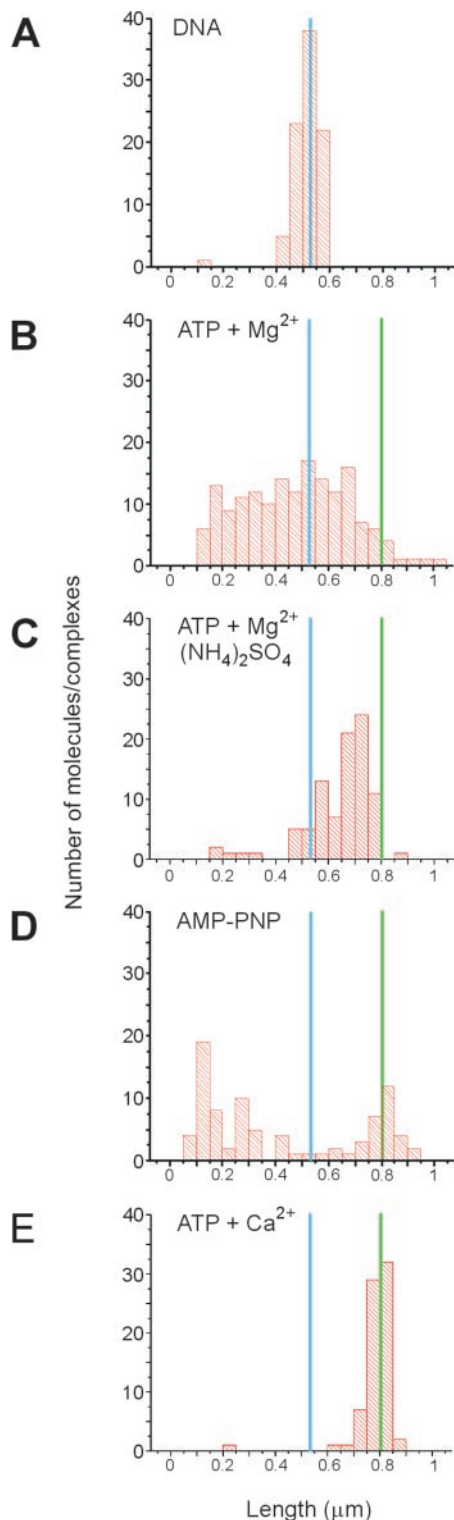
Figure 2. Distribution of filament and DNA lengths measured from SFM images. The length of DNA molecules or filaments in the indicated conditions was measured and their distribution is plotted in histograms. (**A**) Bare DNA without any bound protein. (**B**) Filaments formed by Rad51 in the presence of ATP and MgCl₂. (**C**) Filaments formed by Rad51 in the presence of ATP and MgCl₂ and subsequently treated with $(NH_4)_2SO_4$. (**D**) Filaments formed by Rad51 in the presence of AMP-PNP. (**E**) Filaments formed by Rad51 in the presence of ATP and CaCl₂. The average measured length of the bare DNA fragment (blue line) and the length of this DNA fragment if it is extended 1.5 times in a filament (green line) are indicated in the histograms.

activity was observed in the presence of ATP or ATPγS and Mg^{2+}. Little D-loop formation was detected when ammonium sulfate was added to reactions with ATP and Mg^{2+}. The Rad51 activity measured by D-loop formation does not require ATP hydrolysis as this was most active with the non-hydrolyzable analog AMP-PNP or with ATP and Ca^{2+}, where ATP hydrolysis is considerably inhibited (7). Addition of ammonium sulfate inhibited D-loop formation here, though it has been shown to stimulate Rad51 activity in a different *in vitro* assay [(8) and see Discussion]. The lack of D-loop product correlated with the observation that Rad51 filaments formed on single-stranded DNA in the presence of ATP and Mg^{2+} were disrupted by ammonium sulfate in our experiments.

Dynamic disassembly of human Rad51 filaments correlates with ATP hydrolysis

ATP hydrolysis is required *in vivo* for Rad51 function in homologous recombination (20). We observed that filaments formed in the presence of ATP were very irregular. The irregular structure of these filaments suggested that they might be dynamic, with active exchange of free and DNA-bound Rad51 along the filament. To test if this was the case, we characterized the transition from regular to irregular filaments. Ammonium sulfate does not significantly inhibit the ATPase activity of Rad51 [(14); and data not shown], but does result in the formation of regular filaments. We therefore reasoned that removing ammonium sulfate would provide an experimental tool to control the transition from regular to irregular filaments. For this purpose, filaments were formed with Rad51 and double-stranded DNA in conditions including ATP and Mg^{2+}, followed by addition of ammonium sulfate as before. After deposition onto mica, excess buffer was removed and replaced with a buffer lacking ammonium sulfate and Rad51. The filaments deposited on mica were incubated in this buffer for varying times before observation by SFM. As can be seen in Figure 5A, incubation without ammonium sulfate for 1, 5 and 30 min resulted in increasing disorder along the filaments, apparent loss of protein from DNA and eventually completely protein-free DNA. Filament length also decreased over this time indicating that DNA extension is not maintained as the filaments become irregular (Figure 5B). In contrast to RecA (26), Rad51 dissociation did not occur from one end, but apparently from many sites along the DNA. The effect of ammonium sulfate on stability of the Rad51 filaments was specific and not a general effect of salt in the buffer. Substitution of KCl for ammonium sulfate did not stabilize the filaments, irregular filaments appeared just as in the absence of ammonium sulfate or when it was removed without additional salt (Figure 5D). Incubation of Rad51 filaments on mica *per se* does not result in their dissociation, as regular filaments remained stable in buffer including ammonium sulfate but without Rad51 even after 30 min of incubation (Figure 5C). Though Rad51 binds to DNA in the presence of ADP, irregular filaments were also formed when ADP was used as a cofactor (Figure 5E).

The experiments incubating filaments on mica suggested that filaments disassembled over the course of ∼30 min by dissociation of Rad51 from many points. It is notable that the Rad51 protein in filaments bound to mica appeared to behave the same as it did in solution. The appearance of filaments on
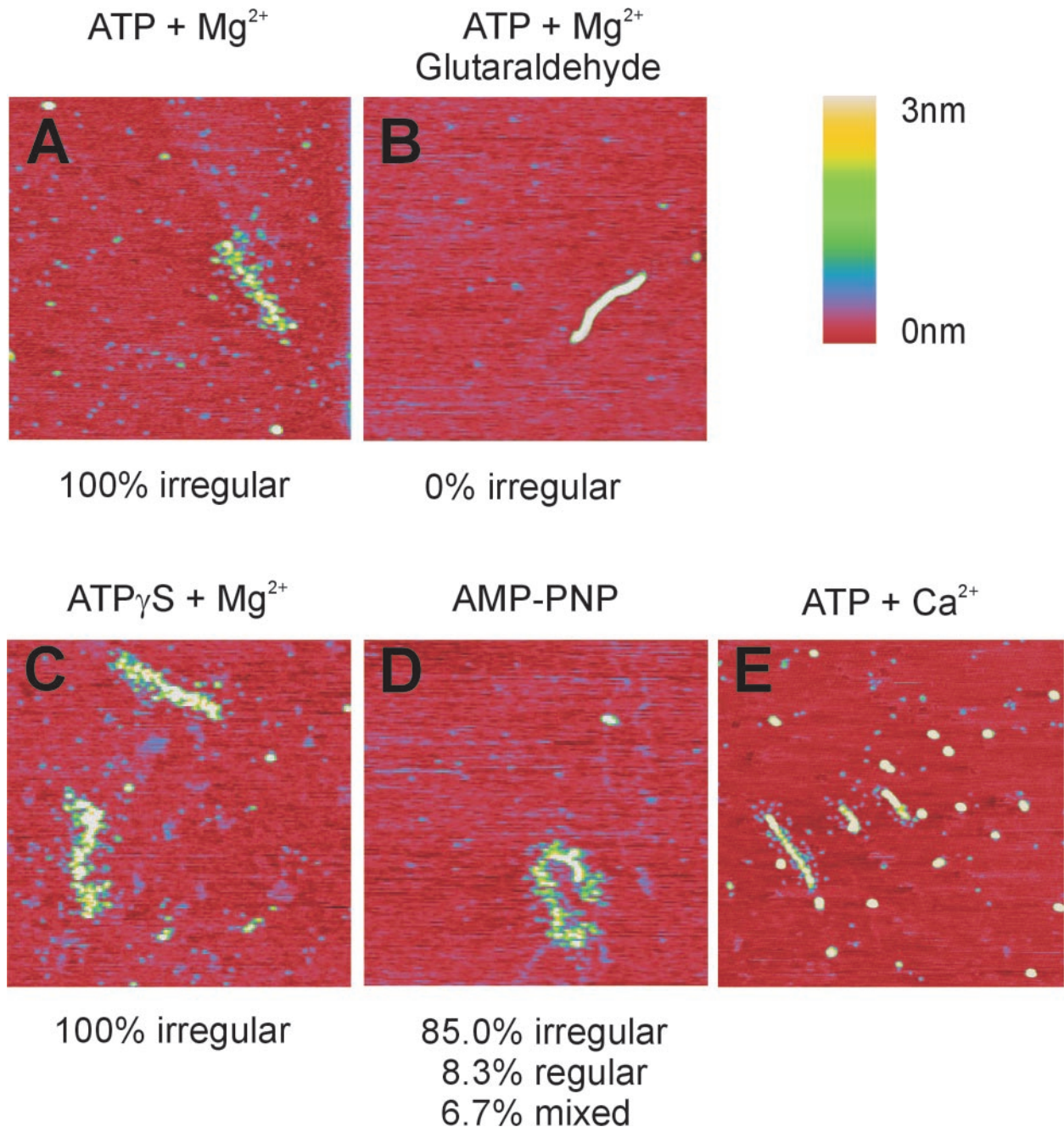
ATP + Mg^{2+} ATP + Mg^{2+}
Glutaraldehyde

3nm

0nm

100% irregular   0% irregular

ATPγS + Mg^{2+} AMP-PNP   ATP + Ca^{2+}

100% irregular   85.0% irregular
8.3% regular
6.7% mixed

Figure 3. SFM images of filaments formed by human Rad51 on single-stranded DNA in the presence of various nucleotide cofactors. Examples of protein–DNA complexes formed on single-stranded DNA in the presence of ATP and MgCl$_2$ deposited directly (**A**) and after fixation with glutaraldehyde (**B**). Examples of filaments formed on single-stranded DNA in the presence of ATPγS (**C**), AMP-PNP (**D**), and ATP and CaCl$_2$ (**E**). The percentage of filaments appearing irregular (such as in A and C) or regular is listed below the images. All images are 1 × 1 μm and height is represented by color in the range of 0–3 nm, red to yellow as shown in the scale bar.

mica after removal of ammonium sulfate was the same as the appearance of filaments deposited from solution reactions including ATP. However, it was not possible to follow these apparent dynamics directly and we could not exclude possible effects of the surface on this reaction and its apparent kinetics.

In order to study the dynamics without possible interference from surface immobilization, we followed Rad51 filament assembly and disassembly on single DNA molecules held in magnetic tweezers. An 8 kb double-stranded DNA molecule

was tethered between a surface and a magnetic bead such that the position of the bead and the force exerted upon it could be manipulated and recorded. In the experiments reported, DNA with at least one nick near the magnetic bead was used, resulting in a torsionally unconstrained DNA molecule. At a constant stretching force, enough to extend the DNA molecule but not distort its structure, the assembly of a Rad51 filament on this DNA will increase the length of the tethered molecule. Assembly (or disassembly) of the filament was followed in
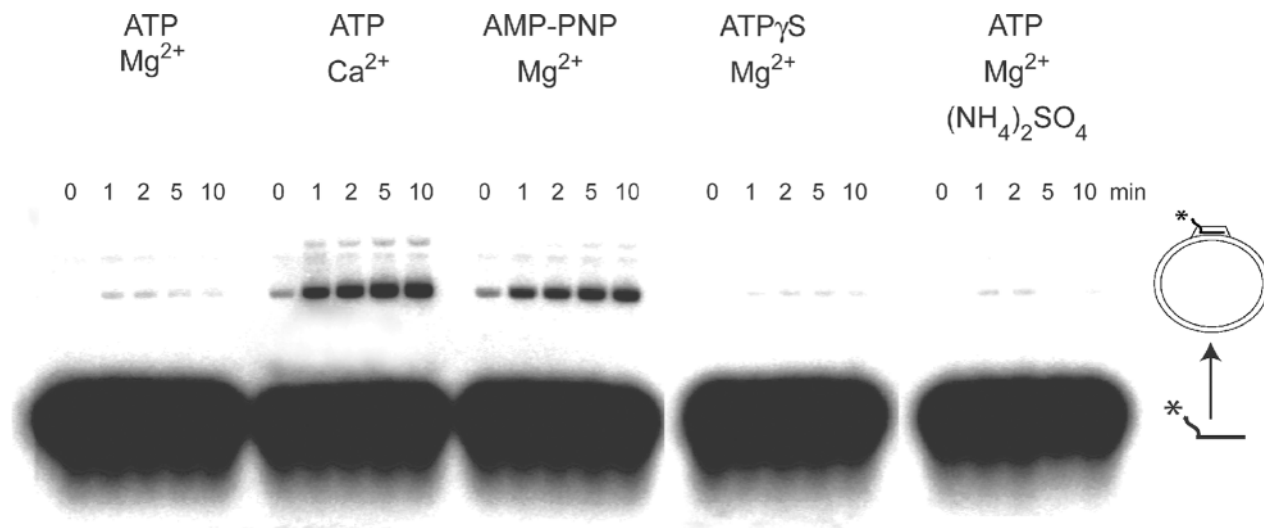
Figure 4. D-loop assay for recombination function. Human Rad51 was incubated with radiolabeled single-stranded oligonucleotide, supercoiled plasmid and the indicated nucleotide cofactors. Oligonucleotide substrates and D-loop recombination products were separated on a gel and the appearance of the D-loop product was followed in time as indicated.

real-time by recording changes in the height of the magnetic bead. Upon addition of buffer containing Rad51, ATP and Mg^{2+}, filament assembly was very fast. The dynamics of this process could not be properly followed when 830 nM Rad51 was added to the flow cell as the DNA tether was already extended to 1.35 times the length of bare DNA when the inflow of Rad51 was stopped (at ~75 s, Figure 6A). This is equivalent to ~70% of the DNA covered by a filament extending the helix 1.5 times its B-form length that had formed while flushing the flow cell. Note that the assembly rate could have been affected by the extra extension of the double-stranded DNA due to the drag of the flow. At lower levels of Rad51, 166 nM added to the flow cell, the dynamics of filament assembly could be separated from flushing the flow cell. However, full extension to 1.5 times the original DNA length was not observed in these conditions (Figure 6B). Very similar time courses, fast assembly for 830 nM Rad51 and slower assembly for 166 nM Rad51 were observed in several independent experiments (3 and 11 respectively).

The non-linear elongation of DNA versus time in the presence of 166 nM Rad51 indicated that the rate-limiting step in filament assembly was not a slow DNA binding or nucleation event followed by more rapid filament growth (Figure 6B). Rather it appeared that nucleation events of Rad51 binding to DNA occurred at multiple sites, the frequency of which depended on the concentration of free Rad51 (a complete quantitative analysis of these and other tweezers experiments will be published elsewhere). Filaments formed in these conditions, continuous presence of Rad51 and ATP, remained stable and elongated, within the detection limits of the tweezers, for several hours. Addition of ammonium sulfate after the formation of filaments did not affect their elongation. However, addition of ammonium sulfate together with Rad51 prevented any obvious filament formation, consistent with SFM imaging of reactions assembled in this way (data not shown). As observed by SFM, elongated filaments were formed when Rad51 was added to the flow cell together with AMP-PNP or with ATP and Ca^{2+} instead of Mg^{2+} (data not shown).

Disassembly of a Rad51–DNA filament formed in the presence of ATP was followed after replacing the buffer in the flow cell with one that lacked ATP and Rad51. The bead height, representing end-to-end distance of the tethered molecule decreased over the course of 50 min to the original length of bare DNA (Figure 6C). The exponential decay of this curve indicated that filament dissociation did not occur from one end or a single point, but that Rad51 dissociated from many points along the molecule. As expected from the SFM imaging experiments, Rad51 filaments treated with ammonium sulfate or formed with ATP and Ca^{2+} did not dissociate when the buffer was replaced with one lacking Rad51 and ATP (observed for several hours to over-night). These single molecule dynamic measurements of filament disassembly in solution confirmed the snap shot SFM images of filament disassembly on mica.

DISCUSSION

We observe that the human recombinase Rad51 forms regular stable filaments with extended double-stranded DNA in conditions that promote an efficient *in vitro* strand exchange reaction (7,8). *In vitro* assays for recombinase functions measure the accumulation of DNA products after de-proteination, thus the conditions that stabilize these double-stranded DNA structures would enhance product accumulation. The regular filament form appears to be trapped when ATP, or a structural mimic, is bound but not hydrolyzed. AMP-PNP is a chemical analog of ATP that can bind to but is not hydrolyzed by ATPases such as Rad51. Substituting Ca^{2+} for Mg^{2+} in reactions involving human Rad51 results in a reduced ATPase rate that maintains human Rad51 in an ATP-bound form (7). The effects of ammonium sulfate are more complex. It is likely that one effect of ammonium sulfate is to mimic an ATP-bound form of Rad51. Although ammonium sulfate does not inhibit the ATPase activity of human Rad51 [(14), and data not shown], it probably does influence conformation at the
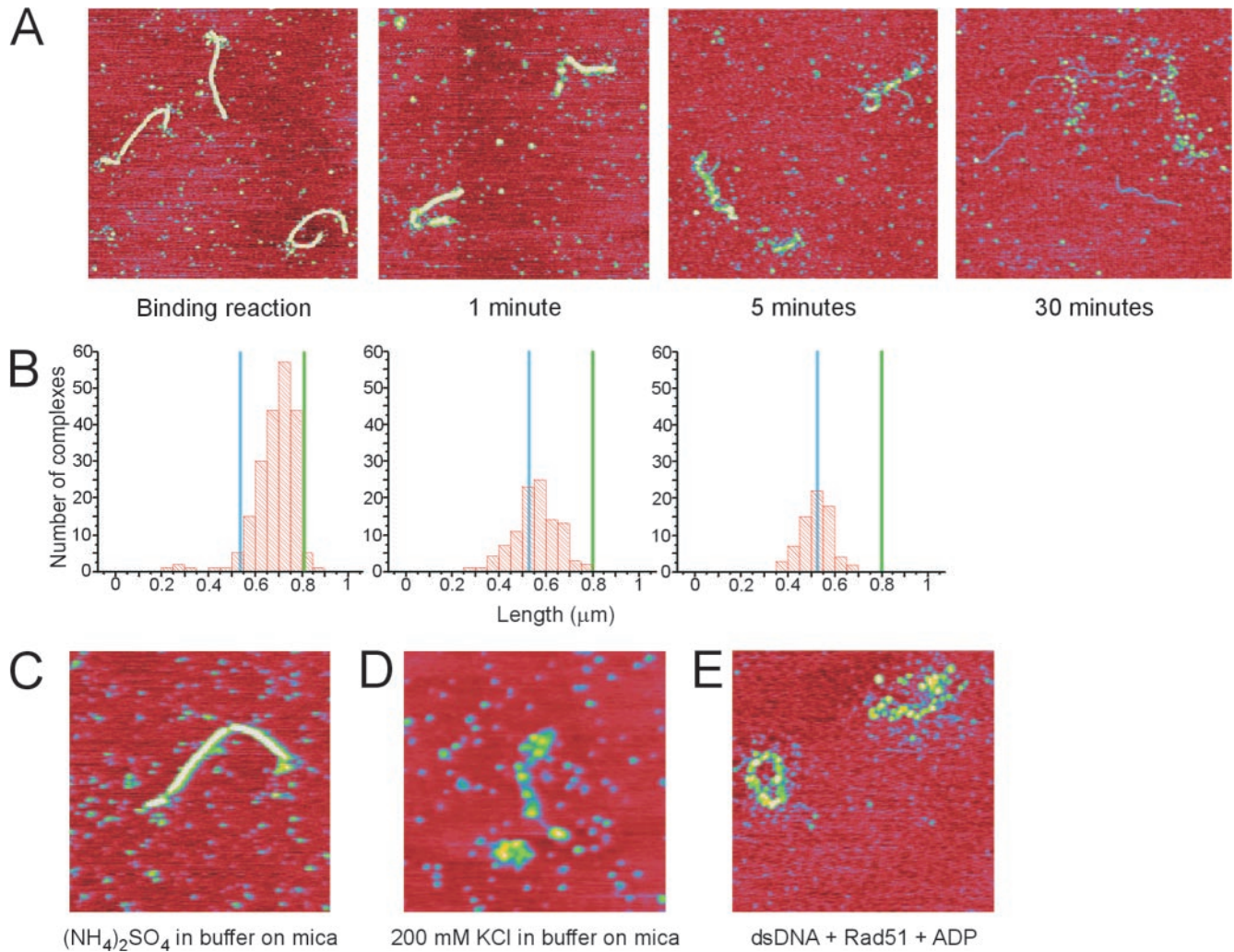
Figure 5. Disassembly of human Rad51 filaments formed on double-stranded DNA in the presence of ATP and MgCl$_2$ treated with (NH$_4$)$_2$SO$_4$ before deposition onto mica for imaging. (**A**) SFM images of filaments from the binding reaction treated with (NH$_4$)$_2$SO$_4$ and deposited (as in Figure 1C), and samples of the same reaction deposited onto mica and incubated on mica in buffer lacking (NH$_4$)$_2$SO$_4$ for the indicated times (1, 5 and 30 min). (**B**) Quantification of filament disassembly on mica presented as histograms of filament lengths measured from the reactions shown in (A). The length of the bare DNA fragment (blue line) and the length of this DNA fragment if it is extended to 1.5 times its length in a filament (green line) are indicated in the histograms. (**C–E**) SFM images of control reactions showing the appearance of filaments formed as indicated: in the presence of ATP and MgCl$_2$ and incubated on mica in buffer including (NH$_4$)$_2$SO$_4$ (C), in the presence of ATP and MgCl$_2$ incubated on mica in buffer including KCl (D), and filaments formed by Rad51 on double-stranded (ds) DNA in the presence of ADP and MgCl$_2$ (E). Images are 1.5×1.5 μM in (A) and 1×1 μM in (C, D and E) and height is represented by color in the range of 0–3 nm, red to yellow.

ATPase active site. The atomic structures of both the archaeal recombinase *Pf*Rad51 (27) and the yeast *Sc*Rad51 (28) have a sulfate ion (presumably scavenged from the crystallization solution), not a nucleotide, bound in their ATPase active sites. Either the bound sulfate ion alone or in the presence of ADP could induce the same protein conformation as bound ATP (14). Additionally, it is expected that ammonium sulfate has a more general role, as increased ionic strength prevents aggregation of Rad51–DNA filaments *in vitro*. Accordingly, incubation with KCl also prevents non-specific aggregation but does not result in regular filaments [(5,8) and Figure 5C].

The importance of nucleotide cofactors for filament structure and stability is clear in the atomic structures of *Sc*Rad51 and *Methanococcus volte* RadA in filaments on DNA (28,29). In these two structures, the ATPase active site is at the junction of adjacent monomers in a filament. In the *Mv*RadA filament structure, the AMP-PNP nucleotide is clearly resolved as a

bridge between adjacent RadA monomers. It is easy to imagine that hydrolysis of ATP would, in simple terms, break this bridge or change the conformation of the adjacent recombinase monomers so that the subunit interface becomes less stable.

The structural requirements for filaments on single-stranded DNA that are needed to form joint molecules are often assumed but have not yet been defined. We observed mostly irregular filaments in all conditions on single-stranded DNA, even in conditions that resulted in most active recombination. Regular filaments have been reported by others in these conditions (5,30), but only after fixation which could have trapped otherwise dynamic protein in a regular structure. Indeed after treatment of half of a reaction that produced irregular filaments on single-stranded DNA with glutaraldehyde, exclusively regular filaments were observed (Figure 3A and B). The irregular appearance of the filaments suggests
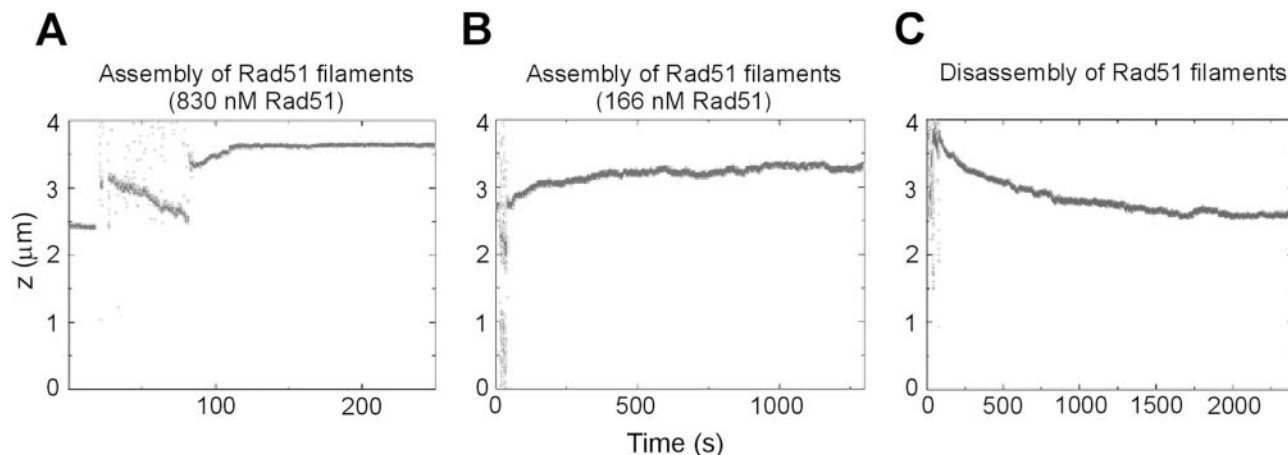
Figure 6. Assembly and disassembly of human Rad51 filaments on double-stranded DNA followed in real-time in a magnetic tweezers setup. (**A**) Time course of a fast filament assembly reaction with 830 nM Rad51. (**B**) Time course of a slow filament assembly reaction with 166 nM Rad51. (**C**) Time course of a Rad51 filament disassembly reaction upon removal of Rad51 and ATP from the flow cell. In all experiments, the DNA tether was held at a constant stretching force of 1.0 pN. Buffer exchange occured for the first 60–75 s.

dynamic association and disassociation of subunits. Our data do not rule out regular filaments as the active species in joint molecule formation, a dynamic transition to short-lived regular forms would explain their rarity. However, it is difficult to imagine the strand exchange steps of homologous recombination occurring without dynamic rearrangement of protein and DNA in the filaments.

The description we provide here of Rad51-DNA filament structure and stability should form the basis for subsequent investigation into the effect of the recombination mediators on dynamic filament assembly and disassembly. The recombination reaction mediated by eukaryotic proteins that can be completed *in vitro* by the bacterial recombinase RecA alone requires, in addition to the recombinase, a host of additional eukaryotic proteins, often called recombination mediators (31,32). The suggested roles of the recombination mediators involve promoting the formation of recombinase filaments and stabilizing appropriately formed filaments on single-stranded DNA. For example, the mediator BRCA2 promotes Rad51 binding to recombination-competent DNA structures (33). Other mediators, the Rad51 paralogs, are suggested to stabilize Rad51-DNA filaments since one of them, human XRCC2, is an ADP/ATP exchange factor for Rad51 that would help maintain Rad51 in an ATP-bound state (34). Rad54 can also stabilize Rad51 filaments on single-stranded DNA (35–37). The transition to unstable and disassembling filaments after joint molecule formation is also a step where the recombination mediators could provide regulation and control.

We followed disassembly of filaments formed on double-stranded DNA, and demonstrated that Rad51 filaments disassembled in conditions that correlate with transition from an ATP to an ADP-bound form of Rad51. Filament disassembly followed on mica suggested that Rad51 monomers disassociate from DNA at multiple places. Quantitative analysis of Rad51 filament disassembly from the single molecule force spectroscopy experiments also indicated that Rad51 disassociation occurred from many places along the molecule. Rad51 apparently nucleates filament formation at many sites along DNA with, we assume, independent initial orientation of monomers probably resulting in filament segments with

opposite polarity running into each other. Our observation of multiple disassembly points could be due to dissociation of Rad51 monomers from internal sites of filaments. However, this could also reflect monomer dissociation exclusively from the ends of many short independently nucleated filaments.

Filament disassembly is likely to be as important as assembly in authentic recombination reactions *in vivo*. *In vitro* assays for recombinase functions measure the accumulation of joint molecule intermediates or strand exchange products after de-proteination, which eliminates any differences among the reactions with respect to disassociation of the recombinase. However, recombination *in vivo* does not stop at joint molecule formation or strand exchange. To complete the process, other proteins need access to the joint molecule to extend the invading strand by polymerization or extend the heteroduplex by Holliday junction migration and eventually to resolve the recombined molecules. A recombinase filament covering the joint molecule is likely to inhibit these processes. Indeed, a dynamic RecA filament, capable of hydrolyzing ATP, is required for *in vitro* recombination coupled replication of *E.coli* (38). Similar replication coupled reactions are essential recombination process in both prokaryotes and eukaryotes (39).

Though our data do not yet address the function of Rad51 filament dynamics for identifying homology or strand invasion, a comparison with another DNA–protein polymer may be informative here. Though the ultimate result is a site-specific, and not a general recombination event, some analogies can be made between the phage Mu transposition reaction and Rad51-mediated recombination, specifically with respect to MuB function and activity. Similar to Rad51, MuB bound to ATP forms polymers on DNA and ATP hydrolysis is coupled to polymer disassembly (40,41). In addition, MuB monomers readily exchange between polymers on DNA in both an end-dependent and end-independent manner (40,42). The MuB-DNA polymer functions to direct the site of phage Mu insertion. It is suggested that the dynamic assembly and disassembly on DNA effectively allow MuB to sample multiple DNA locations until a suitable one is found, a MuB-DNA polymer is formed and remains stable enough for transposition

to proceed (40). Similarly, dynamic Rad51-DNA interactions could result in transiently regular filaments, which would allow Rad51-bound single-stranded DNA to sample for homologous regions in the double-stranded target DNA, thus implying that a regular protein filament would stabilize the formation of a proper duplex joint molecule, promoting heteroduplex extension and favoring further steps of homologous recombination. Formation of a regular protein filament with extended DNA is a required step in current models of homologous recombination. We do not dispute the importance of helical nucleoprotein filaments in eukaryotic homologous recombination, but suggest that important questions remain regarding the functional lifetime of this structure as well as the identity of the reaction step, pre-synaptic or post-synaptic, requiring it.

ACKNOWLEDGEMENTS

REFERENCES

1. DiCapua,E., Engel,A., Stasiak,A. and Kooller,T. (1982) Characterization of complexes between recA protein and duplex DNA by electron microscopy. *J. Mol. Biol.*, **157**, 87–103.
2. Dunn,K., Chrysogelos,S. and Griffith,J. (1982) Electron microscopic visualization of RecA-DNA filaments: evidence for cyclic extension of duplex DNA. *Cell*, **28**, 757–765.
3. Flory,J. and Radding,C.M. (1982) Visualization of RecA protein and its association with DNA: a priming effect of single-strand binding protein. *Cell*, **28**, 747–756.
4. Yu,X., VanLoock,M.S., Yang,S., Reese,J.T. and Egelman,E.H. (2004) What is the structure of the RecA-DNA filament? *Curr. Protein Pept. Sci.*, **5**, 73–79.
5. Liu,Y., Stasiak,A.Z., Masson,J.Y., McIlwraith,M.J., Stasiak,A. and West,S.C. (2004) Conformational changes modulate the activity of human RAD51 protein. *J. Mol. Biol.*, **337**, 817–827.
6. Yu,X., Jacobs,S.A., West,S.C., Ogawa,T. and Egelman,E.H. (2001) Domain structure and dynamics in the helical filaments formed by RecA and Rad51 on DNA. *Proc. Natl Acad. Sci. USA*, **98**, 8419–8424.
7. Bugreev,D.V. and Mazin,A.V. (2004) Ca2+ activates human homologous recombination protein Rad51 by modulating its ATPase activity. *Proc. Natl Acad. Sci. USA*, **101**, 9988–9993.
8. Sigurdsson,S., Trujillo,K., Song,B., Stratton,S. and Sung,P. (2001) Basis for avid homologous DNA strand exchange by human Rad51 and RPA. *J. Biol. Chem.*, **276**, 8798–8806.
9. Namsaraev,E.A. and Berg,P. (1998) Binding of Rad51p to DNA. Interaction of Rad51p with single- and double-stranded DNA. *J. Biol. Chem.*, **273**, 6177–6182.
10. Gupta,R.C., Bazemore,L.R., Golub,E.I. and Radding,C.M. (1997) Activities of human recombination protein Rad51. *Proc. Natl Acad. Sci. USA*, **94**, 463–468.
11. Kim,H.K., Morimatsu,K., Norden,B., Ardhammar,M. and Takahashi,M. (2002) ADP stabilizes the human Rad51-single stranded DNA complex and promotes its DNA annealing activity. *Genes Cells*, **7**, 1125–1134.
12. De Zutter,J.K. and Knight,K.L. (1999) The hRad51 and RecA proteins show significant differences in cooperative binding to single-stranded DNA. *J. Mol. Biol.*, **293**, 769–780.
13. Zaitseva,E.M., Zaitsev,E.N. and Kowalczykowski,S.C. (1999) The DNA binding properties of *Saccharomyces cerevisiae* Rad51 protein. *J. Biol. Chem.*, **274**, 2907–2915.
14. Tombline,G. and Fishel,R. (2002) Biochemical characterization of the human RAD51 protein. I. ATP hydrolysis. *J. Biol. Chem.*, **277**, 14417–14425.
15. Cox,M.M. (2003) The bacterial RecA protein as a motor protein. *Annu. Rev. Microbiol.*, **57**, 551–577.
16. Tombline,G., Heinen,C.D., Shim,K.S. and Fishel,R. (2002) Biochemical characterization of the human RAD51 protein. III. Modulation of DNA binding by adenosine nucleotides. *J. Biol. Chem.*, **277**, 14434–14442.
17. Rehrauer,W.M. and Kowalczykowski,S.C. (1993) Alteration of the nucleoside triphosphate (NTP) catalytic domain within *Escherichia coli* recA protein attenuates NTP hydrolysis but not joint molecule formation. *J. Biol. Chem.*, **268**, 1292–1297.
18. Kowalczykowski,S.C. and Krupp,R.A. (1995) DNA-strand exchange promoted by RecA protein in the absence of ATP: implications for the mechanism of energy transduction in protein-promoted nucleic acid transactions. *Proc. Natl Acad. Sci. USA*, **92**, 3478–3482.
19. Symington,L.S. (2002) Role of RAD52 epistasis group genes in homologous recombination and double-strand break repair. *Microbiol. Mol. Biol. Rev.*, **66**, 630–670.
20. Stark,J.M., Hu,P., Pierce,A.J., Moynahan,M.E., Ellis,N. and Jasin,M. (2002) ATP hydrolysis by mammalian RAD51 has a key role during homology-directed DNA repair. *J. Biol. Chem.*, **277**, 20185–20194.
21. Konola,J.T., Logan,K.M. and Knight,K.L. (1994) Functional characterization of residues in the P-loop motif of the RecA protein ATP binding site. *J. Mol. Biol.*, **237**, 20–34.
22. Ristic,D., Wyman,C., Paulusma,C. and Kanaar,R. (2001) The architecture of the human Rad54-DNA complex provides evidence for protein translocation along DNA. *Proc. Natl Acad. Sci. USA*, **98**, 8454–8460.
23. van der Heijden,T., van Noort,J., van Leest,H., Kanaar,R., Wyman,C., Dekker,N. and Dekker,C. (2005) Torque-limited RecA polymerization on dsDNA. *Nucleic Acids Res.*, **33**, 2099–2105.
24. Mazin,A.V., Zaitseva,E., Sung,P. and Kowalczykowski,S.C. (2000) Tailed duplex DNA is the preferred substrate for Rad51 protein-mediated homologous pairing. *EMBO J.*, **19**, 1148–1156.
25. van Noort,J., Verbrugge,S., Goosen,N., Dekker,C. and Dame,R.T. (2004) Dual architectural roles of HU: formation of flexible hinges and rigid filaments. *Proc. Natl Acad. Sci. USA*, **101**, 6969–6974.
26. Bork,J.M., Cox,M.M. and Inman,R.B. (2001) RecA protein filaments disassemble in the 5′ to 3′ direction on single-stranded DNA. *J. Biol. Chem.*, **276**, 45740–45743.
27. Shin,D.S., Pellegrini,L., Daniels,D.S., Yelent,B., Craig,L., Bates,D., Yu,D.S., Shivji,M.K., Hitomi,C., Arvai,A.S. *et al.* (2003) Full-length archaeal Rad51 structure and mutants: mechanisms for RAD51 assembly and control by BRCA2. *EMBO J.*, **22**, 4566–4576.
28. Conway,A.B., Lynch,T.W., Zhang,Y., Fortin,G.S., Fung,C.W., Symington,L.S. and Rice,P.A. (2004) Crystal structure of a Rad51 filament. *Nature Struct. Mol. Biol.*, **11**, 791–796.
29. Wu,Y., He,Y., Moya,I.A., Qian,X. and Luo,Y. (2004) Crystal structure of archaeal recombinase RADA: a snapshot of its extended conformation. *Mol. Cell*, **15**, 423–435.
30. Benson,F.E., Stasiak,A. and West,S.C. (1994) Purification and characterization of the human Rad51 protein, an analogue of *E.coli* RecA. *EMBO J.*, **13**, 5764–5771.
31. Sung,P., Krejci,L., Van Komen,S. and Sehorn,M.G. (2003) Rad51 recombinase and recombination mediators. *J. Biol. Chem.*, **278**, 42729–42732.
32. Wyman,C., Ristic,D. and Kanaar,R. (2004) Homologous recombination-mediated double-strand break repair. *DNA Repair (Amst.)*, **3**, 827–833.
33. Yang,H., Li,Q., Fan,J., Holloman,W.K. and Pavletich,N.P. (2005) The BRCA2 homologue Brh2 nucleates RAD51 filament formation at a dsDNA–ssDNA junction. *Nature*, **433**, 653–657.
34. Shim,K.S., Schmutte,C., Tombline,G., Heinen,C.D. and Fishel,R. (2004) hXRCC2 enhances ADP/ATP processing and strand exchange by hRAD51. *J. Biol. Chem.*, **279**, 30385–30394.
35. Tan,T.L., Kanaar,R. and Wyman,C. (2003) Rad54, a Jack of all trades in homologous recombination. *DNA Repair (Amst.)*, **2**, 787–794.
36. Mazin,A.V., Alexeev,A.A. and Kowalczykowski,S.C. (2003) A novel function of Rad54 protein. Stabilization of the Rad51 nucleoprotein filament. *J. Biol. Chem.*, **278**, 14029–14036.
37. Wolner,B. and Peterson,C.L. (2005) ATP-dependent and ATP-independent roles for the RAD54 chromatin remodeling enzyme during

recombinational repair of a DNA double strand break. *J. Biol. Chem.*, **280**, 10855–10860.

38. Xu,L. and Marians,K.J. (2002) A dynamic RecA filament permits DNA polymerase-catalyzed extension of the invading strand in recombination intermediates. *J. Biol. Chem.*, **277**, 14321–14328.

39. Cox,M.M., Goodman,M.F., Kreuzer,K.N., Sherratt,D.J., Sandler,S.J. and Marians,K.J. (2000) The importance of repairing stalled replication forks. *Nature*, **404**, 37–41.

40. Greene,E.C. and Mizuuchi,K. (2002) Dynamics of a protein polymer: the assembly and disassembly pathways of the MuB transposition target complex. *EMBO J.*, **21**, 1477–1486.

41. Greene,E.C. and Mizuuchi,K. (2002) Direct observation of single MuB polymers: evidence for a DNA-dependent conformational change for generating an active target complex. *Mol. Cell*, **9**, 1079–1089.

42. Greene,E.C. and Mizuuchi,K. (2004) Visualizing the assembly and disassembly mechanisms of the MuB transposition targeting complex. *J. Biol. Chem.*, **279**, 16736–16743.